



THIS MANUSCRIPT HAS BEEN SUBMITTED TO THE JOURNAL OF GLACIOLOGY AND HAS NOT BEEN PEER-REVIEWED.

### Tracking glacier surge evolution using interferometric SAR coherence – examples from Svalbard

Journal:	<i>Journal of Glaciology</i>
Manuscript ID	JOG-2024-0133.R1
Manuscript Type:	Article
Date Submitted by the Author:	07-Feb-2025
Complete List of Authors:	Schytt Mannerfelt, Erik; University of Oslo Department of Geosciences; University Centre in Svalbard, Arctic Geology Schellenberger, Thomas; University of Oslo Department of Geosciences Kaab, Andreas; University of Oslo Department of Geosciences
Keywords:	Glacier surges, Remote sensing, Ice dynamics
Abstract:	We present a practically simple methodology for tracking glacier surge onset and evolution using interferometric Synthetic Aperture Radar (InSAR) coherence. Detecting surges early and monitoring their build-up is interesting for a multitude of scientific and safety-related aspects. We show that InSAR coherence maps allow the detection of surge-related instability on Svalbard many years before being detectable by, for instance, feature tracking or crevasse detection. Furthermore, we present derived data for two types of surges; down- and up-glacier propagating, with interestingly consistent surge propagation and post-surge relaxation rates. The method works well on Svalbard glaciers, and the data and core principle suggest a global applicability.

SCHOLARONE™  
Manuscripts

# Tracking glacier surge evolution using interferometric SAR coherence — examples from Svalbard

Erik Schytt MANNERFELT,<sup>1,2</sup> Thomas SCHELLENBERGER,<sup>1</sup> Andreas M. KÄÄB<sup>1</sup>

<sup>1</sup>*Department of Geosciences, University of Oslo, Oslo, Norway*

<sup>2</sup>*Arctic Geology, The University Centre in Svalbard, Norway*

*Correspondence: <e.s.mannerfelt@geo.uio.no>*

**ABSTRACT.** We present a practically simple methodology for tracking glacier surge onset and evolution using interferometric Synthetic Aperture Radar (InSAR) coherence. Detecting surges early and monitoring their build-up is interesting for a multitude of scientific and safety-related aspects. We show that InSAR coherence maps allow the detection of surge-related instability on Svalbard many years before being detectable by, for instance, feature tracking or crevasse detection. Furthermore, we present derived data for two types of surges; down- and up-glacier propagating, with interestingly consistent surge propagation and post-surge relaxation rates. The method works well on Svalbard glaciers, and the data and core principle suggest a global applicability.

## 1 INTRODUCTION

Glacier surges are sudden temporary glacier speed-ups, sometimes by one or many orders of magnitudes. Related factors such as substantial mass transfer, change in surface morphology and the time-scale of months to decades are also often included in the definition. The occurrence of this behaviour is concentrated in clusters globally (Sevestre and Benn, 2015; Käääb and others, 2023) with Svalbard being one of these significant clusters. They pose local safety hazards by damming lakes that subsequently outburst (Post and Mayo, 1971; Bazai and others, 2021), or for travel across glaciers, and reveal problems in our understanding of general glacier dynamics due to our inability to properly predict them beforehand. In situ studies of glaciers on the brink of surging yield invaluable information (e.g. Clarke, 1976; Bouchayer and others,

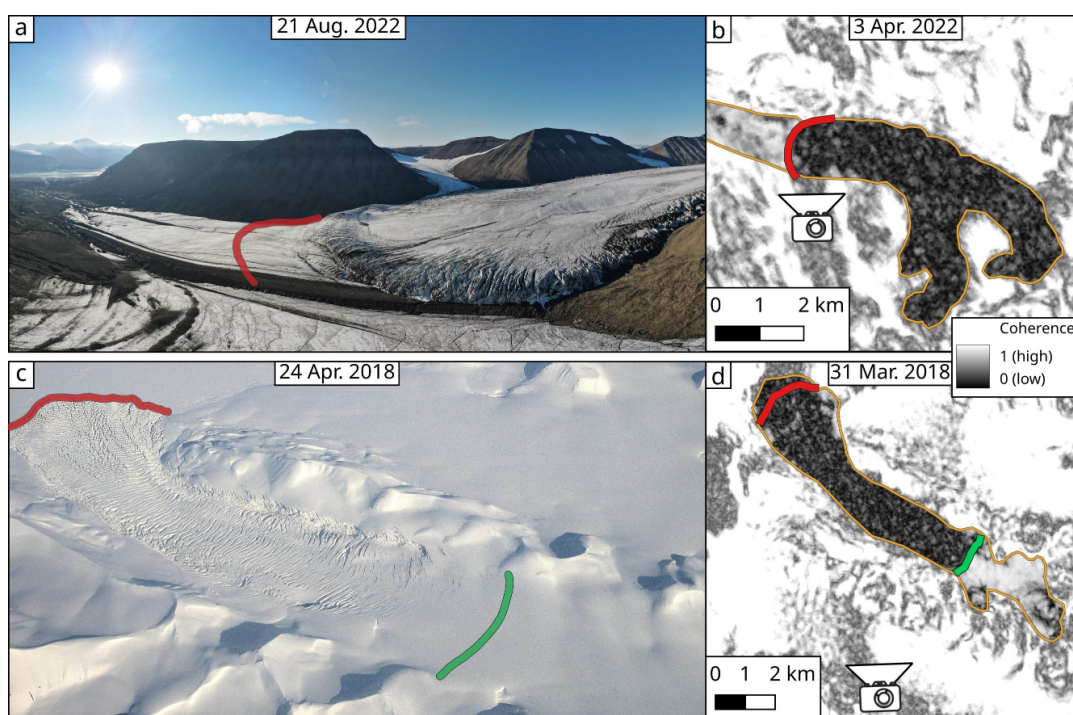


**Fig. 1.** Photographs compared to coherence maps in the same year. **a** Down-glacier propagating surge of Val-låkrabreen, showing a surge bulge with splaying crevasses and a less pronounced forebulge ahead of it (photograph credit: Leonard Magerl). The red line shows the approximate location of the low-coherence boundary from earlier that year (shown in **b**, together with the photo location); roughly coincident with the forebulge. **c** Up-glacier propagating surge of Arnesenbreen (photograph credit: Erik S. Mannerfelt), showing the lower surge boundary in red and the upper low-coherence boundary in green (c.f. panel **d**). We presume that the discrepancy between the green line in **c** and the region of substantial crevassing is due to coherence being sensitive to smaller disturbances than what can be seen in a winter photograph. The largest surge extent (so far) is shown in yellow outlines for panels **b**) and **d**). The dates of the coherence maps represent the latter dates of the acquisition pairs. Areas outside the largest surge extents have reduced contrast to enhance visibility.

26 2024), but the lack of indications before surges means they are generally not known before it is too late to  
 27 study their evolution in entirety. Here, we present a new method for detecting glacier surges years before  
 28 they become detectable by established methods, and demonstrate it on glaciers on Svalbard, presenting  
 29 statistics on the rates of surge evolution throughout the archipelago.

30 Previous methods of surge detection involve identifying sudden changes in geometry, texture or surface  
 31 velocity of a glacier, and we summarize selected studies in the following overview. We focus our background  
 32 contextualisation on detection methods over mechanisms; for an in-depth review on Svalbard surges, we re-  
 33 fer the reader to Harcourt and others (2025). Elevation change maps reveal large mass displacement events  
 34 that can be associated with surge-like instabilities (e.g. Sund and others, 2009; Paul and others, 2022). If  
 35 the surface velocity is high enough, i.e. when a surge has accelerated sufficiently, it can be autonomously  
 36 detected using feature tracking (surface velocity) time series (Koch and others, 2023). Unstable flow such

37 as surging can also be detected by geometrical changes in medial moraines (Herreid and Truffer, 2016).  
38 The detection of drastic increases in crevassing is finally a robust method of identifying an ongoing surge  
39 through subtracting SAR backscatter intensity images over time (Kääb and others, 2023). While all of  
40 these methods work well on their own, they mostly function when the glacier is either fully surging or has  
41 already terminated; characterising the build-up is much more difficult. High-accuracy elevation data can  
42 technically be used over long time periods to reveal unstable mass redistribution associated with future  
43 surging (Sund and others, 2009). Acquiring these elevation data at high accuracy and temporal frequency  
44 requires thorough processing and error assessment, however (c.f. Hugonnet and others, 2022), and finding  
45 an easier and less resource-intensive method would clearly be advantageous.

46 Repeated Synthetic Aperture Radar (SAR) acquisitions of terrain can be used to assess changes in  
47 signal phase, affected by terrain motion, and changes in reflective characteristics. Interferometric SAR  
48 (InSAR), the process of describing these phase changes, is commonly used in cryospheric sciences, e.g for  
49 ground subsidence (Rouyet and others, 2021), glacier velocity (Eldhuset and others, 2003) and classification  
50 of debris-covered glaciers (Thomas and others, 2023). While normal InSAR workflows generally involve  
51 heavy processing to obtain displacement products, a simpler and useful by-product is the normalized cross-  
52 correlation of two single-look complex (SLC) SAR scenes, usually denoted as coherence. InSAR coherence  
53 varies in the range of 0 (no phase correlation between two acquisitions) to 1 (the phase between acquisitions  
54 is identical), and is normally used for quality assessment of the co-registration (Eldhuset and others, 2003),  
55 masking out low-coherence areas within phase unwrapping, and terrain classification (Shi and others, 2019),  
56 including mapping of debris-covered parts of glaciers that are difficult to delineate using optical methods  
57 (Atwood and others, 2010; Frey and others, 2012). Coherence is normally lost either if terrain displacement  
58 or its gradients (acceleration, shear, rotation, etc.) become too large, or if terrain reflective characteristics  
59 change, for example during a rainfall event or during ice- or snowmelt (Weydahl, 2001). Thus, in intervals  
60 featuring stable cold weather, the presence or absence of significant glacier motion, motion gradients, and  
61 deformation can be assessed visually or computationally using InSAR coherence maps. For applications  
62 of InSAR coherence in glacier surging specifically, it has previously been used for masking or quality  
63 assessing InSAR-derived velocity or topographic products (Strozzi and others, 2002), for the indication of  
64 slow surface velocities nearing stagnation (Pritchard and others, 2003), and for a general explanation of  
65 the loss of data beyond a threshold of velocity (Strozzi and others, 2002; Murray and others, 2003a). In  
66 contrast to these previous studies, we consider the loss of coherence as the primary signal in our method,

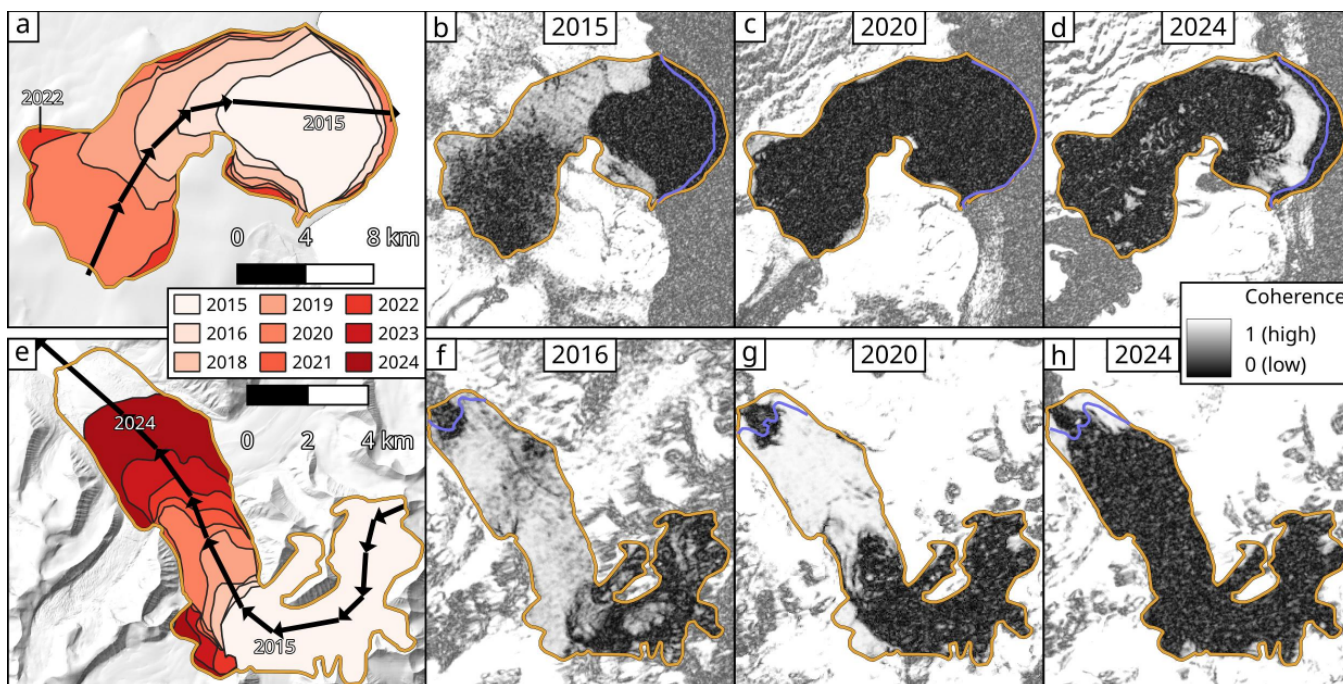


**Fig. 2.** Examples of coherence changes during the progression of two surges. **Top (a–d):** Terminus-initiated surge of Stonebreen. Note the onset of stagnation in 2024 (d) shown by the terminus regaining coherence. **Bottom (e–h):** Surge bulge propagation of Paulabreen. The dates for the latter SAR acquisition in the coherence maps are **b:** 21 January, **c:** 3 March, **d:** 22 March, **f:** 29 March, **g:** 1 April, and **h:** 23 March. The yellow outlines in all panels represent the maximum attained extent of the surges so far, and the blue lines represent the concomitant front positions. Basemap hillshade from 2010 of panels **a** and **e** courtesy of the Norwegian Polar Institute (2014). Areas outside the largest surge extents have reduced contrast to enhance visibility.

67 instead of it acting as an explanatory dataset to contextualize where another product fails.

68 At least a third, and likely much more, of all glaciers on Svalbard have a recent past of surging (Sevestre  
 69 and Benn, 2015; Farnsworth and others, 2016), meaning many currently non-surging glaciers can be de-  
 70 scribed as being in quiescence. Quiescent glacier surface velocities are usually low, measuring  $5\text{--}18\text{ m a}^{-1}$   
 71 on Svalbard (Nuttall and others, 1997; Sund and Eiken, 2004; Sund and others, 2014). Surges dramatically  
 72 elevate this speed to several or tens of metres per day; an order-of-magnitude increase that is well-suited for  
 73 detection. Two types of surge propagation directions have been shown as prevalent on Svalbard (Figure 1);  
 74 down-glacier propagating, characterised by a surface bulge (e.g. Murray and others, 1998), or up-glacier  
 75 propagating, i.e. in a terminus initiated surge (Sevestre and others, 2018). In Alaska, synchronous up- and  
 76 down-glacier propagation of a surge that initiates in the central body has been shown (Altena and others,  
 77 2019), a mechanism that seems rare on Svalbard (Monacobreen; Murray and others, 2003b). We therefore  
 78 focus our present method demonstration on one-directional surge propagation, but our approach could be  
 79 adapted to synchronous up- and down-glacier propagation in the future. Improved monitoring of surge

80 propagation would contribute to better characterising and understanding of the (potentially different) types  
81 of surge evolution and its direction with respect to the direction of glacier flow.

82 We demonstrate the usefulness InSAR coherence maps on Svalbard for tracking down- or up-glacier  
83 propagating surges by mapping out zones of low coherence (disturbed flow) and measuring temporal changes  
84 in their extent. Our resultant patterns show that the technique opens new doors to ways of quantifying  
85 surging, and allows for rough empirical predictions of the timing of surge acceleration. While our study  
86 focuses on Svalbard only, the data and techniques can be used for global assessments of surge propagation  
87 rates and patterns in regions with similarly low quiescent baseline flow.

## 88 **2 DATA AND METHODS**

89 We obtain processed Sentinel-1 inSAR coherence maps from the Alaska Satellite Facility (ASF) Vertex  
90 tool (<https://search.asf.alaska.edu>). We order the processing of every 12-day acquisition pair since  
91 the beginning of the Sentinel-1 record on Svalbard (January 2015) in the winter months of 1 November  
92 to 30 April. We choose this interval as spring or summer melt strongly reduces the phase coherence over  
93 entire glaciers and renders the data unusable for our purposes. Qualitative assessments of 6-day returns  
94 using the Sentinel-1A and -B satellites revealed much cleaner coherence maps, but we stayed consistent  
95 with 12-day baselines as the 6-day availability period lasted only a subset of the study period (Oct. 2016  
96 to Dec. 2021) due to the failure of Sentinel-1B. A total of 797 scenes were successfully processed, with  
97 some failures due to co-registration errors not converging below a threshold (defined in the ASF pipeline).  
98 Most 12-day pairs show very low coherence throughout the scene due to weather effects (Weydahl, 2001).  
99 We sift through the entire catalogue manually for each glacier, and extract at least one suitable coherence  
100 map per year. For each good scene, we manually delineate any encountered low-coherence front with  
101 an upper and/or lower boundary line. A detailed investigation of the influence and the spatio-temporal  
102 variations of factors that contribute to coherence loss at the surge fronts (in particular likely motion  
103 magnitude, motion gradients, surface deformation, and surface changes by crevasse formation) is out of  
104 scope for this brief method demonstration. However, comparison of our coherence-derived surge fronts to  
105 in situ photographs (Figure 1) and DEM differences between occasional individual ArcticDEM products  
106 shows that our coherence-derived surge fronts coincide with topographic bulges, thus indicating a change  
107 in glacier mass transport and dynamics. To obtain terminus positions, we download Sentinel-1 backscatter  
108 intensity and Sentinel-2 L1C true colour scenes for manual terminus delineation. We assess length and

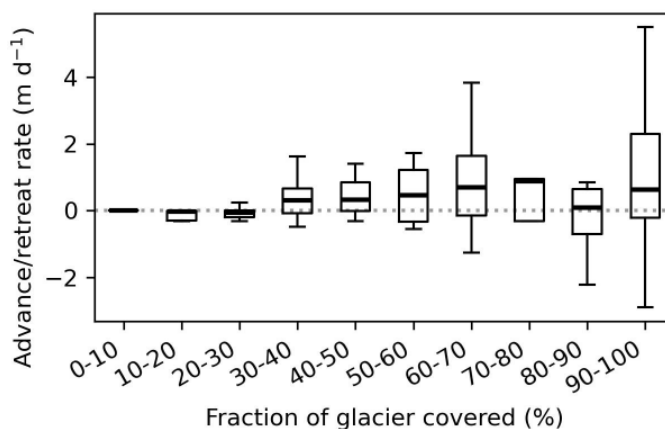


**Fig. 3.** Boxplot comparison of the fraction of low coherence and terminus fluctuation rate at up-glacier propagating (terminus initiated) surges. This was used to derive the 40% threshold as a common starting point for these surges; the 40–50% bin is the first and only bin where the first quartile (the lower box boundary) is above 0 m d<sup>-1</sup>.

109 length change along a manually drawn glacier centreline, measuring the glacier terminus, and the lower and  
 110 upper low-coherence fronts. We measure lengths of parallel lines within a  $\pm 200$  m buffer of the centreline  
 111 to obtain a spread and to reduce uncertainty in the exact placement of the centreline. The chosen buffer  
 112 width of  $\pm 200$  m is open to discussion, but not critical for this method demonstration study. The process  
 113 of our methodology up until this point is summarised in Figure 4.

114 In order to derive further statistics of the mapped surges, we divide them in three stages (if observed);  
 115 pre-surge, surge, and post-surge, based on our available data. The surge onset date is defined differently  
 116 for down- and up-glacier propagating surges. For down-glacier propagating surges, we simply assign the  
 117 latter date of the coherence pair when the low-coherence front (surge bulge) reaches the terminus. Because  
 118 of the sparse temporal resolution of usable coherence maps (most often one or two per year), we cannot  
 119 precisely extract the date of surge onset from this dataset. Therefore, we use the first sign of a frontal  
 120 advance in supplementing Sentinel-1 or -2 images (if there is an advance) after a coherence map date as a  
 121 more precise onset date. For up-glacier propagating surges, we choose a low-coherence expanse threshold  
 122 whereafter the glacier typically starts to advance. As tidewater glaciers often naturally advance in winter  
 123 due to cold waters and sea ice lowering the calving rate (Li and others, 2025), we could not use a simple  
 124 advance rate threshold. We observe that all mapped up-glacier-propagated surging glaciers advanced,  
 125 regardless of season, when 40% or more of the glacier had lost coherence (Figure 3). Thus, we use this  
 126 40% coverage threshold to define the start of an up-glacier propagating surge. An exception is made at  
 127 the glacier Etonbreen as it is part of an ice cap and therefore has an undefined upper bound. Instead,  
 128 we used the date when the glacier first advanced without the help of a sea-ice buffer (November 2023).

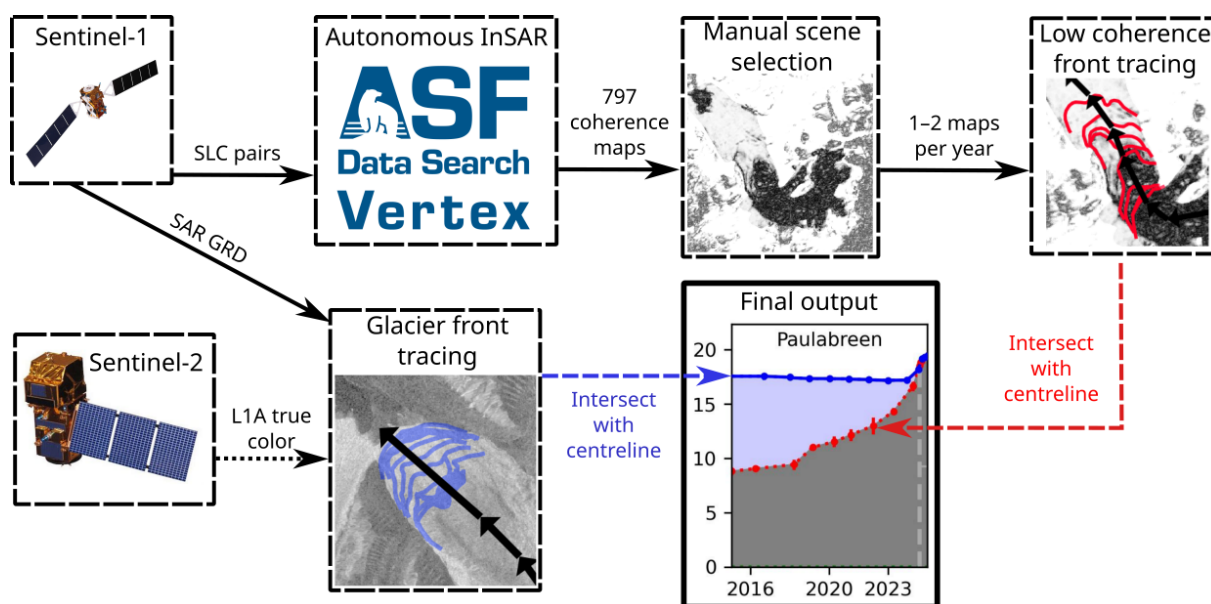


**Fig. 4.** Conceptual diagram of the acquisition and processing of the data. The data examples are from Paulabreen (Figure 2e–h) and showcases the delineation of the lower low-coherence boundary (red) and terminus positions (blue) for its plot in Figure 5e (see that caption for a further explanation of the plot). For up-glacier propagating low-coherence fronts, there is an additional step (green lines, e.g. in Figure 1) to delineate the upper boundary. The latter date in the acquisition pair for the exemplified coherence map ("Manual scene selection" box) is 1 April 2020, and the SAR backscatter image ("Glacier front tracing" box) date is 24 December 2024.

129 The surge termination is defined the same for both types of surges; when the terminus regains coherence  
 130 and thus shows a near or total stagnation at the front. We want to highlight that the exact definition of  
 131 when a surge starts and ends, where it does so, and which indicators are used to define them are all up to  
 132 discussion; we rather see our dates as common "milestone" events along the continuum of surge behaviour.

133 Finally, we test the predictive capability of down-glacier surge progression by fitting a linear model to  
 134 estimate when it will reach the front (Table 1). If the surge has already started within the study period,  
 135 we remove a year's worth of data from before the actual surge onset, to simulate a forecast. We fit a linear  
 136 trend to three of the most recent low coherence boundary measurements (as seen in Figure 5) and solve for  
 137 the date when its length equals the most recent terminus length. We often observe an acceleration right  
 138 before the surge onset, and therefore consider this prediction a latest expected surge date rather than an  
 139 exact one. We observe that the predictions indeed always occur after the true onset, ranging in differences  
 140 from four months at best to nine years at worst.

### 141 3 RESULTS

142 As demonstration of the potential application of our method, we present statistics from 18 glaciers on  
143 Svalbard, including those with recently terminated surges, ongoing surges, or those in the build-up phase.  
144 Out of these, 12 initiated after down-glacier propagation of the low-coherence zone and 6 after up-glacier  
145 propagation. We focus on aggregate statistics here; individual glacier information is found in Table 1.  
146 Unless otherwise specified, the presented numbers show the median $\pm$ standard deviation. We find that  
147 down-glacier propagating surges generally lead to significantly faster terminus advance rates ( $9.2\pm 6.1$   
148  $\text{m d}^{-1}$ ) compared to the up-glacier propagating counterparts ( $0.5\pm 0.4 \text{ m d}^{-1}$ ). However, the low-coherence  
149 front propagation generally shows an opposite tendency, with up-glacier propagation rates of  $4.2\pm 1.8 \text{ m d}^{-1}$   
150 and down-glacier propagation rates of  $2.6\pm 2.3 \text{ m d}^{-1}$ . We qualitatively note an accelerating tendency of  
151 both up- and down-glacier propagation rates near the beginning of the phase when the terminus advances  
152 (Figure 5). There is only a weak correlation between low-coherence front propagation rates and subsequent  
153 advance rates in our data, showing Pearson correlation coefficients of 0.2 and -0.3 for down- and up-glacier  
154 propagating surges, respectively. In other words, there seems to be no simple way to predict the magnitude  
155 of a surge before it accelerates from these data alone.

156 The most consistent measured rate is the gradual return to coherence after a surge. Figure 2d demon-  
157 strates the ongoing stagnation of the recent Stonebreen surge, shown by regained high coherence at the  
158 terminus. All stagnating glaciers in this study show the same pattern of starting at the terminus and grad-  
159 ually continuing up-glacier. This occurs at a rate of  $12.2\pm 4.0 \text{ m d}^{-1}$ , with little to no variability between  
160 down- and up-glacier propagated surges.

### 161 4 DISCUSSION

162 The InSAR coherence loss patterns over time that we exploit in this method test appear to have a close  
163 connection to small changes in ice dynamics that subsequently develop into surges. The promising potential  
164 of this approach is, however, complicated by the fact that most resultant coherence maps (in the maritime  
165 Svalbard climate) are dominated by widespread meteorological coherence losses over the scenes, often  
166 hiding the sought out signal of changes in ice dynamics. Where available, 6-day interferograms show much  
167 higher coherence on Svalbard than the 12-day counterparts that we use here, and the recent successful  
168 replacement of the non-functional Sentinel-1B with Sentinel-1C opens the doors for a continuation of this

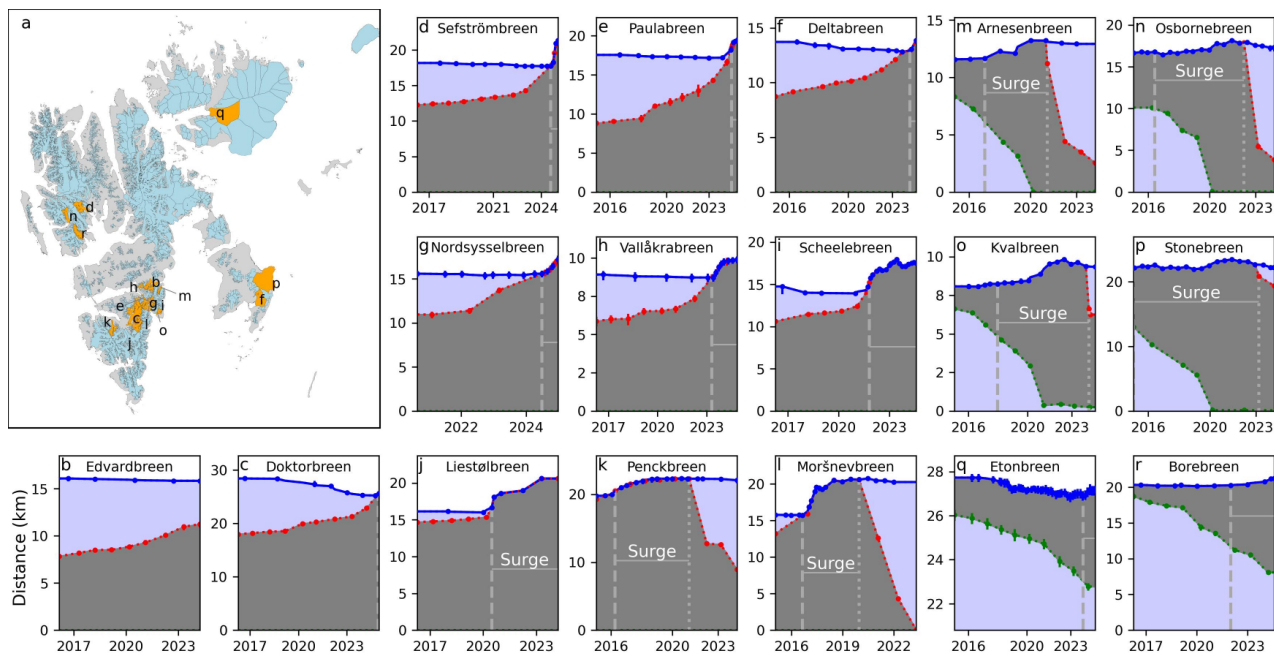


**Fig. 5.** Digitised low-coherence (surge) front progressions for surges on Svalbard. **a**: Overview map showing all glaciers (blue) and the location of the presented glaciers (orange plus letters). Glacier front outlines are from Nuth and others (2013). **b**: Low-coherence front progression that indicates a potential future advance. **c–l**: Down-glacier (bulge) propagating surge examples. **m–r**: Up-glacier (terminus initiated) propagating surge examples. The y-axis represents the total distance along the centreline from the top of the glacier. High-coherence parts of the glacier are shaded light blue, low-coherence parts are shaded grey, front positions are shown in blue, the lower boundary of the low-coherence front in red, and the upper boundary in green. Points (with 25th to 75th percentile spreads) represent measured values, and the parts in between are interpolated. For reference, **c** is lake-terminating, **h**, **i** (before reaching the sea in 2022) and **k** are land-terminating, and the rest are tidewater glaciers.

169 method using 6-day coherence instead. Despite the limitations from meteorological coherence loss and  
 170 availability of certain temporal baselines, the largely uninterrupted Sentinel-1 InSAR coherence time series  
 171 that we exploit represent an impressively consistent and robust data set to track surge evolution in its  
 172 early phases.

173 The identified and described surges in this study display a perhaps surprising similarity in rates and  
 174 patterns of propagation, advance and subsequent stagnation. Most down-glacier propagating surges have  
 175 a well-defined boundary between low and high coherence, with only a few edge cases where shear margins  
 176 (stripes of low coherence) are seen instead (Figure 2). But the similarities should not instil overconfidence  
 177 in the method, as we abandoned the characterisation of the recent surges of Monacobreen (Banerjee and  
 178 others, 2022) and Tunabreen (Vallot and others, 2019); both glaciers are fast-flowing even during quiescence,  
 179 featuring low glacier-wide coherence, and surge propagation monitoring is therefore not possible with our  
 180 method alone. The current implementation of our method is also based on the assumption that a surge  
 181 always eventually leads to an advance. This is not a necessity; the majority of High Mountain Asia surges

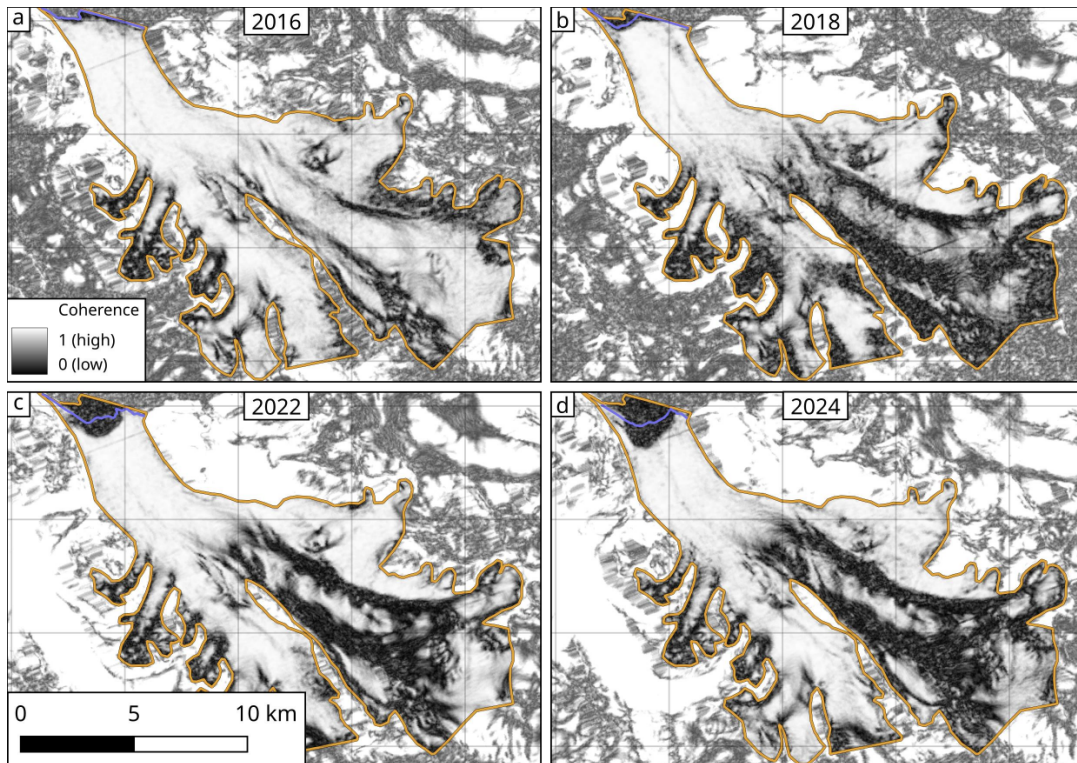


**Fig. 6.** Early surge bulge detection at Kongsvegen, observed visually through changes in InSAR coherence maps. The 5x5 km grid cells show that little progression is observed, but shear margins along the bulge show a progressive reduction in coherence. The yellow outlines in all panels represent the maximum extent of the glacier throughout the study period (2016-), and the blue lines represent the concomitant front positions. The dates for the latter SAR acquisition in the coherence maps are **a**: 10 April, **b**: 19 March, **c**: 3 April, and **d**: 23 March. Areas outside the largest surge extents have reduced contrast to enhance visibility.

182 never reach the terminus (Guillet and others, 2022), and locally confined (also termed incomplete or partial)  
 183 surges have indeed been described as an occasional occurrence on Svalbard as well (Murray and others,  
 184 1998; Sund and others, 2009). While we found no clear indication of a surge that subsided before affecting  
 185 the front over our ten-year study period, we acknowledge the need of an expansion of the surge classification  
 186 scheme for future implementations.

187 An outstanding question in this work is how the initial formation of a down-glacier propagating insta-

**Table 1.** Statistics of the studied down-glacier (↓; bulge) and up-glacier (↑; terminus-initiated) propagating low-coherence fronts. For down-glacier propagating fronts, a linear extrapolation of the surge date from one year prior, shown as "latest surge date". The instability (low-coherence front) propagation rate follows the direction of the surge (up- or down-glacier). The terminus advance rate during the surge, and the post-surge low-coherence front retreat rate (relaxation rate) is presented. The surge advance rate is measured only within one year of the surge starting. Dates are reported in monthly precision to reflect the approximate precision of our measurement.

Glacier	Surge kind	Instability propagation rate (m d <sup>-1</sup> )	Latest surge date	Surge start	Surge advance rate (m d <sup>-1</sup> )	Surge termination	Post-surge relaxation rate (m d <sup>-1</sup> )
Penckbreen	↓	6.9	–	Apr. 2016	4.7	Feb. 2021	8.1
Moršnevbreen	↓	4.2	–	Aug. 2016	9.3	Dec. 2019	12.4
Liestølbreen	↓	2.8	Sep. 2023	Jun. 2020	12.2	–	–
Scheelebreen	↓	6.6	Apr. 2030	Oct. 2021	9.2	–	–
Vallåkrabreen	↓	1.1	Jul. 2025	Apr. 2023	2.6	–	–
Deltabreen	↓	1.2	Sep. 2025	Mar. 2024	3.8	–	–
Nordsyssebreen	↓	3.0	Oct. 2024	Jun. 2024	9.4	–	–
Sefströmbreen	↓	1.5	Dec. 2028	Jul. 2024	16.5	–	–
Paulabreen	↓	5.4	Feb. 2026	Aug. 2024	20.7	–	–
Doktorbreen	↓	2.5	Nov. 2026	Dec. 2024	2.5	–	–
Edvardbreen	↓	1.1	Aug. 2031	–	–	–	–
Kongsvegen	↓	0.2	Sep. 2051	–	–	–	–
Stonebreen	↑	5.0	–	Jan. 2015	0.3	Mar. 2023	6.4
Osbornebreen	↑	5.2	–	Jun. 2016	0.7	Apr. 2022	17.5
Arnesenbreen	↑	5.2	–	Jan. 2017	0.9	Feb. 2021	13.7
Kvalbreen	↑	2.1	–	Dec. 2017	0.2	Feb. 2024	12.0
Borebreen	↑	3.5	–	Jan. 2022	0.3	–	–
Etonbreen	↑	0.8	–	Nov. 2023	1.3	–	–

188 bility looks like. In other words, how far back in time can we detect a future down-glacier propagating  
189 surge? We only have vague indications of initial bulge formation; low-coherence lines associated with shear  
190 margins gradually lose coherence and subsequently start progressing down-glacier. This is exemplified at  
191 the surge of Paulabreen in Figure 2, where the 2016 scene displays only partial loss of coherence in the  
192 surge front, while the latter scenes show a total loss. This type of proto-bulge can be seen in other examples  
193 throughout Svalbard (Figure 6), and might represent the earliest detectable stage of unstable flow through  
194 this method. While interpretations turn vague too far back in time, we still see that many surges can be  
195 seen up to (and maybe longer than) eight years before they reach the front. Thus, mapping the progression  
196 of low-coherence zones on glaciers can be used as an early warning system for many surges.

197 We do not mean to convey that all cases of lost coherence mean that a surge is about to happen.  
198 Persistent low-coherence zones that could be misclassified as surge bulges are found all over Svalbard,  
199 and are most easily explained through uneven variations in subglacial topography leading to local high  
200 flow gradients and thus a reduction in coherence. In addition, all tidewater glaciers seem to feature a  
201 low-coherence zone near their termini, explainable by a steepening and acceleration leading to large defor-  
202 mation and crevassing near their calving bays (Murray and others, 2003a). What differentiates a potential  
203 surge from both of these cases in the coherence is the temporal progression; an expanding disturbance  
204 or an accelerating large terminal low-coherence zone indicates a state change in the glacier's local flow  
205 characteristics. Therefore, we are confident that all our presented examples represent actual surges, but  
206 we may have missed smaller instability progressions that got lost between all other more natural zones of  
207 low to no coherence.

## 208 **5 CONCLUSION**

209 Here, we present InSAR coherence maps as a new tool to track glacier surge evolution from its buildup  
210 phase to stagnation. While the method is only proven to work on glaciers with low baseline quiescent  
211 velocities, the ones we study show clear similarities in surge evolution rates. There is a strong case for  
212 future automation of the tool to detect surge-like glacier flow instabilities, as the ones mapped in this study  
213 are clearly visible in the coherence data with the naked eye. We could infer glacier surges many years (in one  
214 case up to eight) before they reached the front, supporting the potential use of the method for safety-related  
215 or scientific forecasting of surge-like behaviour. We believe that the method can provide new insights into  
216 the physics and evolution of glacier surges, for instance regarding the spatio-temporal patterns of initial

ice-flow change. For example, our (limited) study for Svalbard suggests that the instability propagation during the build-up phase has no direct correlation with the magnitude of a later surge, meaning the physics that drive them might be different. As another potentially important result, we want to highlight that the instability propagation that eventually led to surging started many years before accelerating and advancing. This has implications for studies that investigate connections between meteorological or climatic conditions and glacier surging, as a substantial time delay between build-up conditions and the subsequent surge might have to be considered. We thus suggest the use of this simple method as a complement to the existing suite of methods for detecting, mapping, classifying and tracking surges and other surge-like glacier flow instabilities.

## DATA AVAILABILITY

The source code for InSAR post-processing and figures are found at <https://github.com/erikmannerfelt/IncoherentSurges>. Sentinel-1 InSAR products like coherence maps can be requested for free within a quota (as of February 2025) at <https://search.asf.alaska.edu>. Before the potential acceptance and publication of this manuscript, an associated Zenodo publication will be made and linked here with supporting output data.

## ACKNOWLEDGEMENTS

TS was financed by the Research Council of Norway (“Researcher Project for Scientific Renewal”, MASSIVE, Project 315971). AK acknowledges support from the European Space Agency projects Glaciers\_cci and EarthExplorer 10 Harmony (4000127593/19/I-NB, 4000146464/24/NL/MG/ar).

## REFERENCES

- Altena B, Scambos T, Fahnestock M and Kääb A (2019) Extracting recent short-term glacier velocity evolution over southern Alaska and the Yukon from a large collection of Landsat data. *The Cryosphere*, **13**(3), 795–814, ISSN 1994-0424 (doi: 10.5194/tc-13-795-2019)
- Atwood DK, Meyer F and Arendt A (2010) Using L-band SAR coherence to delineate glacier extent. *Canadian Journal of Remote Sensing*, **36**(sup1), S186–S195, ISSN 0703-8992, 1712-7971 (doi: 10.5589/m10-014)
- Banerjee D, Garg V and Thakur PK (2022) Geospatial investigation on transitional (quiescence to surge initiation)

- 243 phase dynamics of Monacobreen tidewater glacier, Svalbard. *Advances in Space Research*, **69**(4), 1813–1839, ISSN  
244 02731177 (doi: 10.1016/j.asr.2021.08.020)
- 245 Bazai NA, Cui P, Carling PA, Wang H, Hassan J, Liu D, Zhang G and Jin W (2021) Increasing glacial lake outburst  
246 flood hazard in response to surge glaciers in the Karakoram. *Earth-Science Reviews*, **212**, 103432, ISSN 00128252  
247 (doi: 10.1016/j.earscirev.2020.103432)
- 248 Bouchayer C, Nanni U, Lefeuvre PM, Hult J, Steffensen Schmidt L, Kohler J, Renard F and Schuler TV (2024)  
249 Multi-scale variations of subglacial hydro-mechanical conditions at Kongsvegen glacier, Svalbard. *The Cryosphere*,  
250 **18**(6), 2939–2968, ISSN 1994-0424 (doi: 10.5194/tc-18-2939-2024)
- 251 Clarke GK (1976) Thermal Regulation of Glacier Surging. *Journal of Glaciology*, **16**(74), 231–250, ISSN 0022-1430,  
252 1727-5652 (doi: 10.3189/S0022143000031567)
- 253 Eldhuset K, Andersen PH, Hauge S, Isaksson E and Weydahl DJ (2003) ERS tandem InSAR processing for DEM  
254 generation, glacier motion estimation and coherence analysis on Svalbard. *International Journal of Remote Sensing*,  
255 **24**(7), 1415–1437, ISSN 0143-1161, 1366-5901 (doi: 10.1080/01431160210153039)
- 256 Farnsworth WR, Ingólfsson O, Retelle M and Schomacker A (2016) Over 400 previously undocumented Svalbard  
257 surge-type glaciers identified. *Geomorphology*, **264**, 52–60, ISSN 0169555X (doi: 10.1016/j.geomorph.2016.03.025)
- 258 Frey H, Paul F and Strozzi T (2012) Compilation of a glacier inventory for the western Himalayas from satellite  
259 data: methods, challenges, and results. *Remote Sensing of Environment*, **124**, 832–843, ISSN 00344257 (doi:  
260 10.1016/j.rse.2012.06.020)
- 261 Guillet G, King O, Lv M, Ghuffar S, Benn D, Quincey D and Bolch T (2022) A regionally resolved inventory of High  
262 Mountain Asia surge-type glaciers, derived from a multi-factor remote sensing approach. *The Cryosphere*, **16**(2),  
263 603–623, ISSN 1994-0424 (doi: 10.5194/tc-16-603-2022)
- 264 Harcourt WD, Pearce DM, Gajek W, Lovell H, Luckman A, Benn D, Kohler J, Käab A and Hann R (2025) Surging  
265 glaciers in Svalbard: Current knowledge and perspectives for monitoring (SvalSurge). Technical report, Svalbard  
266 Integrated Arctic Earth Observing System (doi: 10.5281/ZENODO.14425522)
- 267 Herreid S and Truffer M (2016) Automated detection of unstable glacier flow and a spectrum of speedup behavior  
268 in the Alaska Range. *Journal of Geophysical Research: Earth Surface*, **121**(1), 64–81, ISSN 2169-9003, 2169-9011  
269 (doi: 10.1002/2015JF003502)
- 270 Hugonnet R, Brun F, Berthier E, Dehecq A, Mannerfelt ES, Eckert N and Farinotti D (2022) Uncertainty analysis  
271 of digital elevation models by spatial inference from stable terrain. *IEEE Journal of Selected Topics in Applied*  
272 *Earth Observations and Remote Sensing*, 1–17, ISSN 1939-1404, 2151-1535 (doi: 10.1109/JSTARS.2022.3188922)

- 273 Kääb A, Bazilova V, Leclercq PW, Mannerfelt ES and Strozzi T (2023) Global clustering of recent glacier surges  
274 from radar backscatter data, 2017–2022. *Journal of Glaciology*, 1–9, ISSN 0022-1430, 1727-5652 (doi: 10.1017/jog.  
275 2023.35)
- 276 Koch M, Seehaus T, Friedl P and Braun M (2023) Automated Detection of Glacier Surges from Sentinel-1 Surface  
277 Velocity Time Series—An Example from Svalbard. *Remote Sensing*, **15**(6), 1545, ISSN 2072-4292 (doi: 10.3390/  
278 rs15061545)
- 279 Li T, Hofer S, Moholdt G, Igneczi A, Heidler K, Zhu XX and Bamber J (2025) Pervasive glacier retreats across Sval-  
280 bard from 1985 to 2023. *Nature Communications*, **16**(1), 705, ISSN 2041-1723 (doi: 10.1038/s41467-025-55948-1)
- 281 Murray T, Dowdeswell JA, Drewry DJ and Frearson I (1998) Geometric evolution and ice dynamics during a surge  
282 of Bakaninbreen, Svalbard. *Journal of Glaciology*, **44**(147), 263–272, ISSN 0022-1430, 1727-5652 (doi: 10.3189/  
283 S0022143000002604)
- 284 Murray T, Luckman A, Strozzi T and Nuttall AM (2003a) The initiation of glacier surging at Fridtjovbreen, Svalbard.  
285 *Annals of Glaciology*, **36**, 110–116, ISSN 0260-3055, 1727-5644 (doi: 10.3189/172756403781816275)
- 286 Murray T, Strozzi T, Luckman A, Jiskoot H and Christakos P (2003b) Is there a single surge mechanism? Contrasts  
287 in dynamics between glacier surges in Svalbard and other regions: IS THERE A SINGLE SURGE MECHANISM?  
288 *Journal of Geophysical Research: Solid Earth*, **108**(B5), ISSN 01480227 (doi: 10.1029/2002JB001906)
- 289 Norwegian Polar Institute (2014) Terrengmodell Svalbard (S0 Terrengmodell) (doi: 10.21334/npolar.2014.dce53a47)
- 290 Nuth C, Kohler J, König M, von Deschwanden A, Hagen JO, Kääb A, Moholdt G and Pettersson R (2013) Decadal  
291 changes from a multi-temporal glacier inventory of Svalbard. *The Cryosphere*, **7**(5), 1603–1621, ISSN 1994-0424  
292 (doi: 10.5194/tc-7-1603-2013)
- 293 Nuttall AM, Hagen JO and Dowdeswell J (1997) Quiescent-phase changes in velocity and geometry of Finster-  
294 walderbreen, a surge-type glacier in Svalbard. *Annals of Glaciology*, **24**, 249–254, ISSN 0260-3055, 1727-5644 (doi:  
295 10.3189/S0260305500012258)
- 296 Paul F, Piermattei L, Treichler D, Gilbert L, Girod L, Kääb A, Libert L, Nagler T, Strozzi T and Wuite J (2022)  
297 Three different glacier surges at a spot: what satellites observe and what not. *The Cryosphere*, **16**(6), 2505–2526,  
298 ISSN 1994-0424 (doi: 10.5194/tc-16-2505-2022)
- 299 Post A and Mayo LR (1971) Glacier dammed lakes and outburst floods in Alaska. USGS Numbered Series 455, U.S.  
300 Geological Survey (doi: 10.3133/ha455)

- 301 Pritchard H, Murray T, Strozzi T, Barr S and Luckman A (2003) Surge-related topographic change of the glacier  
302 Sortebræ, East Greenland, derived from synthetic aperture radar interferometry. *Journal of Glaciology*, **49**(166),  
303 381–390, ISSN 0022-1430, 1727-5652 (doi: 10.3189/172756503781830593)
- 304 Rouyet L, Karjalainen O, Niittynen P, Aalto J, Luoto M, Lauknes TR, Larsen Y and Hjort J (2021) Environmen-  
305 tal Controls of InSAR-Based Periglacial Ground Dynamics in a Sub-Arctic Landscape. *Journal of Geophysical*  
306 *Research: Earth Surface*, **126**(7), ISSN 2169-9003, 2169-9011 (doi: 10.1029/2021JF006175)
- 307 Sevestre H and Benn DI (2015) Climatic and geometric controls on the global distribution of surge-type glaciers:  
308 implications for a unifying model of surging. *Journal of Glaciology*, **61**(228), 646–662, ISSN 0022-1430, 1727-5652  
309 (doi: 10.3189/2015JoG14J136)
- 310 Sevestre H, Benn DI, Luckman A, Nuth C, Kohler J, Lindbäck K and Pettersson R (2018) Tidewater Glacier Surges  
311 Initiated at the Terminus. *Journal of Geophysical Research: Earth Surface*, **123**(5), 1035–1051, ISSN 21699003  
312 (doi: 10.1029/2017JF004358)
- 313 Shi Y, Liu G, Wang X, Liu Q, Zhang R and Jia H (2019) Assessing the Glacier Boundaries in the Qinghai-Tibetan  
314 Plateau of China by Multi-Temporal Coherence Estimation with Sentinel-1A InSAR. *Remote Sensing*, **11**(4), 392,  
315 ISSN 2072-4292 (doi: 10.3390/rs11040392)
- 316 Strozzi T, Luckman A, Murray T, Wegmuller U and Werner C (2002) Glacier motion estimation using SAR offset-  
317 tracking procedures. *IEEE Transactions on Geoscience and Remote Sensing*, **40**(11), 2384–2391, ISSN 0196-2892  
318 (doi: 10.1109/TGRS.2002.805079)
- 319 Sund M and Eiken T (2004) Quiescent-phase dynamics and surge history of a polythermal glacier: Hessbreen,  
320 Svalbard. *Journal of Glaciology*, **50**(171), 547–555, ISSN 0022-1430, 1727-5652 (doi: 10.3189/172756504781829666)
- 321 Sund M, Eiken T, Hagen JO and Kääb A (2009) Svalbard surge dynamics derived from geometric changes. *Annals*  
322 *of Glaciology*, **50**(52), 50–60, ISSN 0260-3055, 1727-5644 (doi: 10.3189/172756409789624265)
- 323 Sund M, Lauknes TR and Eiken T (2014) Surge dynamics in the Nathorstbreen glacier system, Svalbard. *The*  
324 *Cryosphere*, **8**(2), 623–638, ISSN 1994-0424 (doi: 10.5194/tc-8-623-2014)
- 325 Thomas DJ, Robson BA and Racoviteanu A (2023) An integrated deep learning and object-based image analysis  
326 approach for mapping debris-covered glaciers. *Frontiers in Remote Sensing*, **4**, 1161530, ISSN 2673-6187 (doi:  
327 10.3389/frsen.2023.1161530)
- 328 Vallot D, Adinugroho S, Strand R, How P, Pettersson R, Benn DI and Hulton NRJ (2019) Automatic detection of  
329 calving events from time-lapse imagery at Tunabreen, Svalbard. *Geoscientific Instrumentation, Methods and Data*  
330 *Systems*, **8**(1), 113–127, ISSN 2193-0864 (doi: 10.5194/gi-8-113-2019)

- 331 Weydahl D (2001) Analysis of ERS Tandem SAR coherence from glaciers, valleys, and fjord ice on Svalbard. *IEEE*  
332 *Transactions on Geoscience and Remote Sensing*, **39**(9), 2029–2039, ISSN 01962892 (doi: 10.1109/36.951093)

For Peer Review